

# Hydroxyl Defect Effect on Reoxidation of Sc-Doped (Ba,Ca)(Ti,Zr)O<sub>3</sub> Fired in Reducing Atmospheres

Yu-Ju Kao,<sup>‡</sup> Che-Yi Su,<sup>§</sup> Christian Pithan,<sup>§</sup> Detlev F. Hennings,<sup>§</sup> Chi-Yuen Huang,<sup>‡,†</sup> and Rainer Waser<sup>¶,§</sup>

<sup>‡</sup>Department of Resources Engineering, National Cheng Kung University, Tainan 70101, Taiwan

<sup>§</sup>Peter Grünberg Institut, PGI-7: Electronic Materials, Forschungszentrum Jülich GmbH, D-52425 Jülich, Germany

<sup>¶</sup>Institut für Werkstoffe der Elektrotechnik II, RWTH Aachen, D-52056 Aachen, Germany

**The behavior of grain and grain-boundary conductivity of acceptor (Sc)-doped (Ba,Ca)(Ti,Zr)O<sub>3</sub> ceramics sintered in moist reducing atmosphere and subsequently reoxidized in dry and moist atmosphere was investigated by means of impedance spectroscopy (IS). In moist firing atmosphere, water vapor was found to react with oxygen vacancies, forming positively charged hydroxyl defects (OH)<sub>0</sub><sup>•</sup> on regular oxygen sites in the crystal lattice. Proton hopping is considered to raise the ionic conductivity significantly. Therefore, hydroxyl defects (OH)<sub>0</sub><sup>•</sup> in turn influence the grain conduction. Hydroxyl defects (OH)<sub>0</sub><sup>•</sup> are also considered to be responsible for alternations of the dielectric maximum at the Curie point.**

## I. Introduction

THE trend of electronic industry is toward miniaturization. Multilayer ceramic capacitors (MLCCs) in products have to decrease their size and enhance volumetric capacitance efficiency. BaTiO<sub>3</sub> is the dielectric constituent of commercial MLCCs owing to its extremely high dielectric constant associated with a series of ferroelectric phase transitions. MLCCs with Ni internal electrodes are produced on a mass scale composed of hundreds of dielectric layers of 1 μm and less in thickness for high capacitance devices. Ni-MLCCs are commonly fired in reducing environment of moist mixtures of nitrogen and hydrogen (N<sub>2</sub>/H<sub>2</sub> + H<sub>2</sub>O) to prevent the oxidation of the Ni internal electrodes. In such reducing atmospheres, BaTiO<sub>3</sub> forms a large amount of positively charged oxygen vacancies, V<sub>O</sub><sup>•</sup>, defects that are electrically compensated by a high number of conduction electrons<sup>1,2</sup>, which give rise to a dramatic decline of the insulation resistance (IR) by 10 to 12 orders of magnitude. Herbert et al.<sup>3</sup> discovered that the re-establishment of a high IR by addition of certain transition-metal ions to semiconducting BaTiO<sub>3</sub> is possible. Daniels<sup>2</sup> found that the transition-metal ions such as Fe<sup>3+</sup>, Mn<sup>2+</sup>, and Cr<sup>3+</sup> act as strong electron acceptors on Ti-sites.

An ongoing issue in the industrialization of Ni-MLCCs was the suppression of the electrical degradation, which depends sensitively on the oxygen activity during processing. The IR of acceptor-doped Ni-MLCCs under direct-current (dc) bias breaks down abruptly after a few hours. A rather high mobility of oxygen vacancies in the electric field was considered to be responsible for the phenomenon of electrical

degradation.<sup>4</sup> The most critical issue for acceptor-doped Ni-MLCCs is electrical degradation, which is ascribed to a large amount of oxygen vacancies in the dielectric materials.

A slight reoxidation treatment, at temperatures between approximately 900°C and 1000°C within an atmosphere containing only very little oxygen, improved definitely the life reliability of Ni-MLCCs.<sup>5</sup> To prevent the Ni inner electrodes from oxidation, the oxygen partial pressure during reoxidation must be kept low enough. The effect of reoxidation on the life reliability improvement of Ni-MLCCs was plausibly attributed to the reduction in the number of oxygen vacancies.<sup>6</sup> As for the commonly used valence instable acceptor ions, e.g., Mn<sup>3+</sup> or Cr<sup>3+</sup>, reoxidation induces a valence change, e.g., Mn<sup>3+</sup> to Mn<sup>4+</sup>, thus diminishing the number of compensating oxygen vacancies. However, the low oxygen partial pressure of oxygen  $p(\text{O}_2)$  of  $5 \times 10^{-11}$  bar at 1000°C for the Ni/NiO equilibrium, provided by the Ni inner electrodes, limits the reoxidation process.<sup>7</sup> Large numbers of oxygen vacancies therefore remain after the reoxidation process. Moreover, valence stable acceptors,<sup>8–11</sup> such as Ca<sup>2+</sup>, and rare-earth metal ions, such as Y<sup>3+</sup>, Sc<sup>3+</sup>, Dy<sup>3+</sup>, and Ho<sup>3+</sup> on the Ti-site do not alter their valence state. Therefore, the number of compensating oxygen vacancies remains unchanged after reoxidation.

Impedance spectroscopy (IS) is a powerful technique to study the electrical and dielectric properties of ceramics as it allows to distinguish the intrinsic (bulk) properties from extrinsic contributions associated with grain boundaries, surface layers, and electrode interfaces.<sup>12</sup> Previous impedance spectroscopic (IS) experiments on Yb<sup>3+</sup>- and Sc<sup>3+</sup>-doped (Ba,Ca)(Ti,Zr)O<sub>3</sub> (BCTZ) material<sup>13</sup> revealed frequency tuned relaxation phenomena typical for grain-boundary barrier layers. IS measurements detected three different relaxation steps in reoxidized Yb-doped BCTZ ceramics within the frequency range from 10 mHz to 10 MHz at 250°C.<sup>13</sup> These steps were assigned to the RC-regimes of the grains, of the grain boundaries, and of the electrode interfaces, respectively. Moreover, Yang et al.<sup>14</sup> also identified double Schottky barriers at grain boundaries and electrodes interfaces in Ni-MLCCs. The activation energies, being higher than for the bulk, were lowered under DC-bias voltage.

Coufova et al.<sup>15</sup> found hydroxyl defects by observing OH-stretch vibrations in BaTiO<sub>3</sub> single crystals. Stotz et al.<sup>16</sup> reported about hydroxyl defects replacing oxygen ions O<sup>2-</sup> in the sublattices of oxides as positively charged donors (OH)<sub>0</sub><sup>•</sup>. Hennings et al.<sup>17</sup> found that hydroxyl defects, existing in freshly prepared hydrothermal BaTiO<sub>3</sub> powders, could be removed as desorbed water on heating in air at temperatures above 300°C. Waser<sup>18</sup> studied absorption and desorption of D<sub>2</sub>O (heavy water) in BaTiO<sub>3</sub> at 900°C. A strongly increasing solubility of (OD)<sub>0</sub><sup>•</sup> defects with increasing number of ionized oxygen vacancies could be detected, corre-

E. C. Dickey—contributing editor

Manuscript No. 36342. Received February 3, 2015; approved December 1, 2015.

<sup>†</sup>Author to whom correspondence should be addressed. e-mail: cyhuang@mail.ncku.edu.tw

sponding to increasing concentration of acceptors. A negligible amount of oxygen vacancies and, respectively, negligible solubility of  $(\text{OD})_{\text{O}}^{\bullet}$  were observed in donor-doped  $\text{BaTiO}_3$ . Therefore, a strong relation between the formation of hydroxyl defects and oxygen vacancies was deduced. The effect of hydroxyl defects incorporated into the perovskite lattice is also expected to modify the dielectric characteristics in acceptor-doped dielectric ceramics fired in moist atmosphere. Rare-earth acceptor-doped  $(\text{Ba,Ca})(\text{Ti,Zr})\text{O}_3$  ceramics fired in reductive atmosphere showed pronounced changes of the dielectric characteristics after reoxidation.<sup>19</sup> The height of the dielectric Curie maximum and the dissipation losses were significantly influenced by various treatments in dry and moist atmosphere.<sup>20</sup>

A notable ionic conductivity was found in  $\text{BaTiO}_3$  with an applied electrical field due to the high mobility of ionized oxygen vacancies.<sup>21</sup> Hydroxyl ions  $(\text{OH})_{\text{O}}^{\bullet}$  are considered to be too large for electromigration. On the contrary, protons  $\text{H}^+$  could move as interstitial defects through the oxygen sublattice easily. Proton hopping, i.e., proton diffusion through proton displacement, is therefore assumed to give rise to a considerable contribution to the ionic conduction in  $\text{BaTiO}_3$ , in addition to electromobility of charged oxygen vacancies. Protonic defects in acceptor-doped perovskite-type oxides have been studied in detail;<sup>22</sup> however, this study seems to be not comprehensive enough to clearly understand the effect of moisture on the resulting proton conductivity in the materials of Ni-MLCCs.

The purpose of this study is to investigate the difference in relaxation characteristics and dielectric properties in Sc-doped dielectric ceramics of the system  $(\text{Ba,Ca})(\text{Ti,Zr})\text{O}_3$  (BCTZ), which have been fired under moist reducing conditions and afterwards reoxidized at 1000°C in various moist and dry atmospheres. It is well-known that the ionic size is a main factor influencing the incorporation of rare-earth ions into BT ceramics.<sup>23–28</sup> The ionic radii of Ti (0.605 Å), Zr (0.72 Å), and Sc (0.745 Å) are quite similar.<sup>29</sup> Sc ions will therefore preferentially occupy the B-site to act as acceptors. Slight excess of BaO guarantees exclusive incorporation on B-sites.<sup>10</sup>

## II. Experimental Procedure

### (1) Sample Preparation

Dielectric powders of the nominal composition  $(\text{Ba}_{0.96}\text{Ca}_{0.04})(\text{Ti}_{0.8125}\text{Sc}_{0.0075}\text{Zr}_{0.18})\text{O}_3$  were prepared by the conventional solid-state reaction method, using reagent-grade  $\text{BaCO}_3$ ,  $\text{CaCO}_3$ ,  $\text{TiO}_2$ ,  $\text{Sc}_2\text{O}_3$ , and  $\text{ZrO}_2$  as raw materials. A slight excess of 0.5 mol% of the A-site ion  $\text{Ba}^{2+}$  was employed in this formulation in order to assure the incorporation of the  $\text{Sc}^{3+}$  ion as  $\text{Sc}_{\text{Ti}}^{\prime}$  acceptor on the Ti-site. Similar compositions are commonly used in connection with the industrial production of dielectric materials showing the temperature specification of Y5V and a dielectric maximum at a temperature of approximately 20°C. Before weighing,  $\text{BaCO}_3$  was dried at 700°C for 1 h in  $\text{CO}_2$ ,  $\text{Sc}_2\text{O}_3$  and  $\text{TiO}_2$  were dried at 600°C for 1 h in  $\text{O}_2$ ,  $\text{ZrO}_2$  was dried at 500°C for 1 h in  $\text{O}_2$ , and  $\text{CaCO}_3$  was dried at 400°C for 1 h in  $\text{CO}_2$  to ensure the compositional accuracy. The raw materials were intensively blended, mixed, and milled for 24 h in a suspension with isopropanol (solid content: 40%), using a polyethylene jar and  $\text{Y}_2\text{O}_3$ -stabilized  $\text{ZrO}_2$  balls. The ball-milled slurries were then dried in a rotary evaporator and thereafter pulverized with an agate mortar before calcination. Calcination treatments were conducted at 1200°C for 5 h in air. The calcined powders were mixed with 1 mol%  $\text{SiO}_2$  as sintering aid, then ground in isopropanol using a planetary mill, followed by 24 h ball-milling. The powders obtained from the dried slurries were then granulated with PVA (Polyvinyl Alcohol) and pressed into disks applying an uniaxial pressure of 400 MPa. After burning out the PVA binder at 400°C for

2 h in air, the disks were sintered at 1360°C for 1 h in a moisturized gas mixture of Ar with 1 vol% of  $\text{H}_2$  that was saturated with water at 20°C. The fired pellets were cut into disks of 10 mm diameter and 0.5 mm thickness with a diamond wire saw and thereafter subjected for 2 h to a reoxidation treatment at 1000°C in various atmospheres of wet and dry mixtures of  $\text{N}_2$  with 50 ppm of  $\text{O}_2$  or wet and dry mixtures of  $\text{N}_2$  or Ar with 20 vol% of  $\text{O}_2$  (synthetic air). The values for the partial pressures of oxygen were shown in Table I. H. Katsu<sup>30</sup> indicated that an oxygen vacancy would only need 0.2 s to migrate at 900°C along a diffusion path of 20  $\mu\text{m}$  by using  $d = \sqrt{D(T) \times t}$ , where  $d$  is the diffusion path length,  $D(T)$  is the diffusion coefficient, and  $t$  is the equilibration time. Therefore, soaking at 1000°C with 2 h is sufficient for defect chemical equilibria during reoxidation in this study. The specimens were slowly cooled down in the furnace in the reoxidation atmosphere. According to the slow cooling in the sluggish furnace, it is expected that water vapor can penetrate the ceramics for a longer period at temperatures below 500°C. No difference of oxygen partial pressures between wet and dry conditions could be measured by a calibrated oxygen sensor. The microstructure of polished and thermally etched ceramics surface was observed using scanning electron microscopy (SEM, S4100, Hitachi, Ibaraki, Japan).

According to the hydration experiments on rare-earth doped  $\text{BaZrO}_3$  of Kreuer et al.,<sup>22</sup> a saturation of the ceramics with water vapor,  $p(\text{H}_2\text{O}) = 23$  mbar, can be expected at  $T < 400^\circ\text{C}$ . The temperature dependence of water uptake is determined by the kind and concentration of the acceptor dope as well as by the basic composition of the perovskite.

Figure 1(a) and (b) show microstructures of as-fired Sc-BCTZ ceramics sintered in moist reducing atmosphere and additionally reoxidized at 1000°C in dry  $\text{N}_2$  with 50 ppm  $\text{O}_2$ . The grain sizes are about 5  $\mu\text{m}$  in all specimens and the sintering densities of all specimens were approximately 97% of the theoretical density of 6.07 g/cm<sup>3</sup>. These results show that the subsequent reoxidation treatment has insignificant effect on the densities and grain size of specimens.

### (2) Electrical Characterization

As-fired and reoxidized disks were sputtered with Ni electrodes (50 nm thickness) on both sides. Platinum (50 nm thickness) protective layers were sputtered on the top of the Ni-electrodes in order to prevent the oxidation of Ni during the electrical measurements. Impedance analyses were performed on as-fired and annealed ceramics at frequencies from 10 mHz to 10 MHz and at temperatures in the range between  $-60^\circ\text{C}$  and  $300^\circ\text{C}$  using a Novocontrol impedance analyzer (Alpha-Analyzer, Novocontrol GmbH, Montabaur, Germany). The evaluation of each  $R$  (resistance),  $Q$  (constant phase element), and  $n$  (the relaxation distribution parameter ranging from zero to unity) for a properly assumed equivalent circuit and data analysis was carried out using the Zview (Scribner Associates Inc., Southern Pines, NC) software, which extracts  $R$ ,  $Q$ , and  $n$  by nonlinear least-squares (NLLS) fitting. Dielectric temperature characteristics were determined at 1V-ac and 1 kHz in the same temperature interval as requested by the industrial standard Y5V for

**Table I. Partial Oxygen Pressure of Various Heat-Treatment Conditions**

Heat-treatment condition		$p_{\text{O}_2}$ (atm)
As fired	Wet	$3.9 \times 10^{-10}$
Reox. 50 ppm $\text{O}_2/\text{N}_2$	Wet	$2.9 \times 10^{-4}$
Reox. 50 ppm $\text{O}_2/\text{N}_2$	Dry	$2.5 \times 10^{-4}$
Reox. air ( $\text{O}_2/\text{N}_2$ )	Wet	$1.7 \times 10^{-1}$

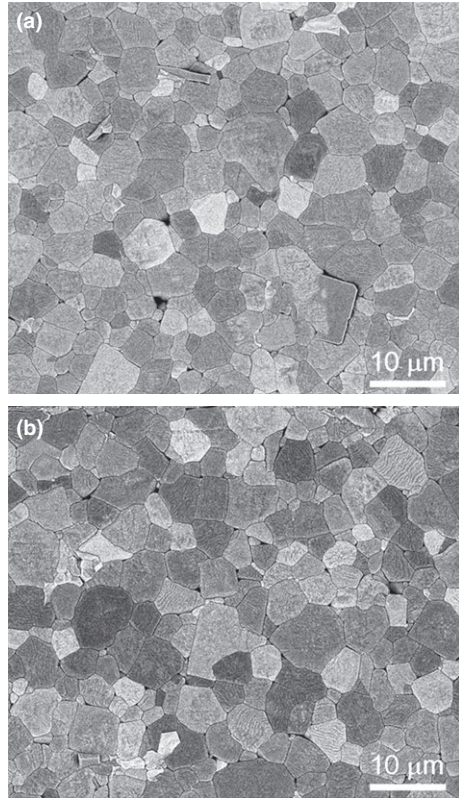


**Fig. 1.** Microstructure of (a) ceramics sintered at 1360°C for 1 h in moist 1 vol% H<sub>2</sub>/Ar (b) additionally reoxidized at 1000°C for 2 h in dry 50 ppm O<sub>2</sub>/N<sub>2</sub>.

dielectric ceramics of MLCCs. The dielectric constant of such material is generally identified at 1 kHz.

### III. Results and Discussion

#### (1) Impedance Spectra Obtained from as-fired and reoxidized Sc-BCTZ Specimens are listed below:

1. Sc-doped BCTZ as fired in moist atmosphere,
2. After additional reoxidation in moist N<sub>2</sub>, 50 ppm O<sub>2</sub>,
3. After additional reoxidation in moist synthetic air,
4. After additional reoxidation in dry N<sub>2</sub>, 50 ppm O<sub>2</sub>.

These IS measurements recorded at 300°C are shown in Fig. 2. An enlarged representation of the results, obtained for specimens treated in moist atmospheres, is shown in the inset of Fig. 2. In the impedance spectra, it is noted that all complex impedance plots consist of two semicircular arcs at higher frequencies and an uncompleted arc at low frequencies in specimens treated in moist atmosphere. Compared to the results represented in Fig. 2, the total DC resistance of the specimens treated in a dry atmosphere is a multitude higher than the specimens that are treated in a moist atmosphere. The shape of the locus curves is apparently affected by the presence of water. The low-frequency branch inclined at approximately 45° seen from the IS spectra of moist atmosphere treated specimens is very likely associated with charge build-up at the blocking metal electrodes.<sup>31</sup> Thus, it is thought that oxygen vacancies are blocked at the electrode–ceramic interfaces, where the electronic conduction is reversible.<sup>32,33</sup> The features at higher frequencies are due to the presence of both grain and grain-boundary contributions in the bulk. The impedance data can be replotted in the electric modulus formalism, as shown in Figs. 3(a)–(c). In the modulus, the height of each peak is proportional to 1/C, and so information about thin layers, such as the electrode and intergranular effects, will tend to be suppressed. Thus, the visible peak in the modulus spectrum is considered reason-

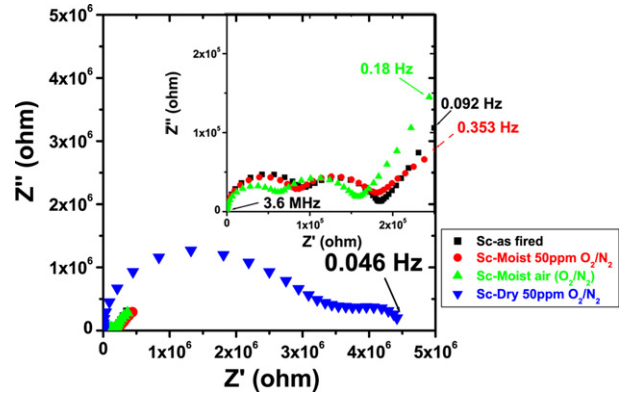


**Fig. 2.** Plots of complex impedance change recorded at 300°C of Sc-BCTZ ceramics sintered in moist reducing atmosphere (black open circle) and reoxidized in various dry and moist atmospheres (colored closed geometrical patterns).

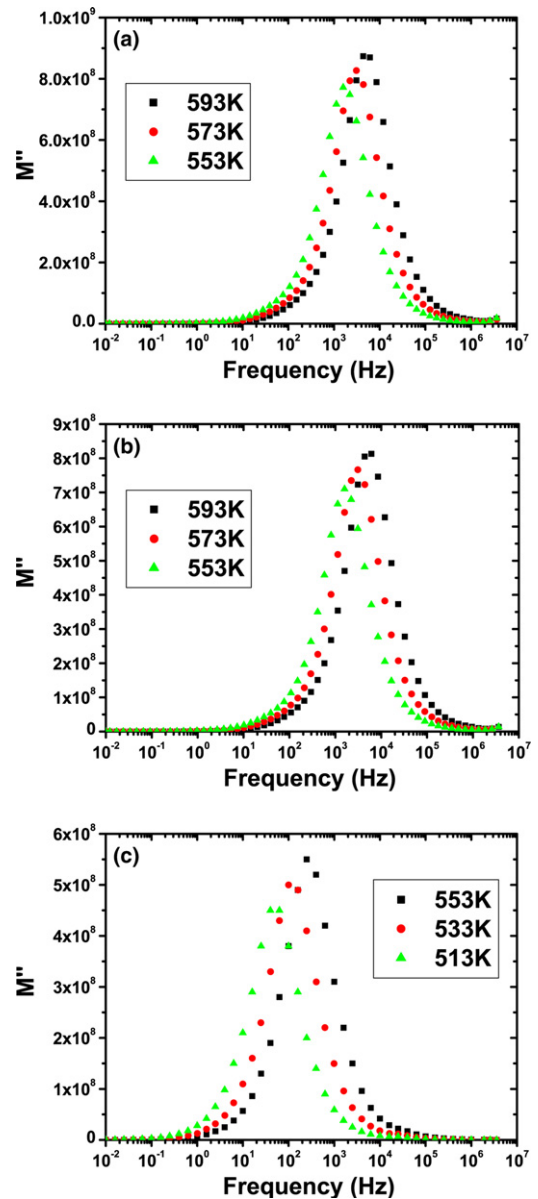


**Fig. 3.** Electric modulus spectra of (a) ceramics sintered at 1360°C for 1 h in moist 1 vol% H<sub>2</sub>/Ar, (b) additionally reoxidized in moist N<sub>2</sub> with 50 ppm O<sub>2</sub>, and (c) additionally reoxidized in dry N<sub>2</sub> with 50 ppm O<sub>2</sub>.



ably to be the response of grain. Furthermore, the frequency of peak maxima in  $M''$  spectroscopic plots is given by the relation:<sup>34,35</sup>

$$2 \times \pi \times f_{\max} \times R \times C = 1 \quad (1)$$

The  $R \times C$  product for each peak is fundamental parameter as also is the value of  $f_{\max}$ . As a result, the peaks in Fig. 3(c) occur at much lower frequency than those in Figs. 3(a) and (b) are ascribed to the higher  $R \times C$  product under dry condition. Regarding the temperature dependence of the peak height in the modulus spectrum, this is grain characteristic of ferroelectric material above Curie temperature, that is, grain capacitance decreases with increasing temperatures.

A core-shell microstructure strongly affects the conduction path of current flows. The current must pass through the region of the resistive shell in series with the conductive core region and the electrode, but it may avoid regions of the shell in parallel with the core leading to an inhomogeneous current density within the microstructure. This will influence the  $R$  and  $C$  values extracted for the core and shell regions. Therefore, it is expected that a double  $M''$  maximum is observed in  $M''$  spectroscopic plots if the time constant,  $\tau = R \times C$  for the regions, differs by at least two orders of magnitude allowing the responses to be resolved in the IS data.<sup>36</sup> However, only a single  $M''$  peak is observed in this study, no significant evidence for core-shell structures, neither in the as-fired condition [Fig. 3(a)] nor in the reoxidized state [Figs. 3(b) and (c)], independently from the postsintering annealing ambient.

## (2) Hydroxyl Defects in Sc-BCTZ Ceramics

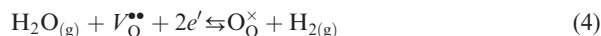
As seen in Fig. 2, all specimens treated during firing or reoxidation in a moist atmosphere, showed a conductivity which was by 1–2 orders of magnitude higher than that of specimens treated in dry atmosphere. The pronounced influence of moisture on the impedance spectra of Sc-BCTZ suggests a strong impact of hydroxyl defects  $(\text{OH})_{\text{O}}^{\bullet}$  on the electrical and dielectric response of Sc-BCTZ ceramics. A distinct relation between the formation of proton defects, acceptors and oxygen vacancies is assumed. In Ba-excess  $\text{BaTiO}_3$  containing  $\text{Sc}^{3+}$ , these ions enter the Ti sites of the perovskite lattice as acceptors:<sup>10</sup>



By the incorporation of  $\text{H}_2\text{O}$ , the oxygen vacancies are partially annihilated and charge compensation is accomplished by the formation of  $(\text{OH})_{\text{O}}^{\bullet}$  defects. No change in the donor defect concentration on the oxygen sites occurs. Absorption and desorption of water in  $\text{BaTiO}_3$  is a reversible reaction:



A further equation for the incorporation of  $\text{H}_2\text{O}$  on the oxygen vacancies of  $\text{BaTiO}_3$  was established by Kessel et al.<sup>37</sup>



No  $(\text{OH})_{\text{O}}^{\bullet}$  defects are formed. Reaction (4) was ruled out, since it is considered as not valid under the present conditions of reoxidation.

Proton hopping is assumed to give a considerable contribution to the ionic conduction in  $\text{BaTiO}_3$ , in addition to electromobility of charged oxygen vacancies.

## (3) Impedance Spectroscopy Analysis for as-fired and reoxidized Sc-BCTZ Ceramics

To further investigate the variation in the grain and grain-boundary conduction in bulk Sc-BCTZ, fired under moist reducing conditions and subsequently reoxidized at  $1000^\circ\text{C}$  in various moist and dry atmospheres, a conventional equivalent circuit was used to model the impedance spectra in this study is shown in Fig. 4 (inset). The model is composed of two  $RQ$ -components of grain and grain boundary, where  $Q$  is constant phase element. By fitting the measured impedance data with these elements, the resistances  $R_{\text{grain}}$  and  $R_{\text{g.b.}}$ , the constant phase elements  $Q_{\text{grain}}$  and  $Q_{\text{g.b.}}$ , and the relaxation distribution parameters  $n_{\text{grain}}$  and  $n_{\text{g.b.}}$  can be evaluated. The capacitance value can also be obtained from the following equation:<sup>38,39</sup>

$$C = (R^{1-n} \times Q)^{1/n} \quad (5)$$

The grain resistivity ( $\rho = 1/\sigma$ ) is defined as:

$$\rho_{\text{grain}} = R_{\text{grain}} \times \frac{A_{\text{eff}}}{L_{\text{eff}}} \quad (6)$$

where  $A_{\text{eff}}$  is the effective cross-sectional area and  $L_{\text{eff}}$  is the effective thickness of ceramics. The grain-boundary resistivity ( $\rho_{\text{g.b.}} = 1/\sigma_{\text{g.b.}}$ ) can be expressed as:

$$\rho_{\text{g.b.}} = R_{\text{g.b.}} \times \frac{C_{\text{g.b.}}}{\epsilon_0 \times \epsilon_{\text{g.b.}}} \quad (7)$$

where  $\epsilon_0$  and  $\epsilon_{\text{g.b.}}$  is the dielectric constant of vacuum and grain boundary, respectively. By using the reasonable approximation of  $\epsilon_{\text{grain}} \approx \epsilon_{\text{g.b.}}$ , the grain-boundary resistivity can be expressed as

$$\rho_{\text{g.b.}} = \frac{R_{\text{g.b.}} \times C_{\text{g.b.}}}{\epsilon_0 \times \epsilon_{\text{grain}}} = \frac{R_{\text{g.b.}} \times C_{\text{g.b.}}}{R_{\text{grain}} \times C_{\text{grain}}} \times \rho_{\text{grain}} \quad (8)$$

Therefore, grain capacitance ( $C_{\text{grain}}$ ), grain-boundary capacitance ( $C_{\text{g.b.}}$ ), grain conductivity ( $\sigma_{\text{grain}}$ ), and grain-boundary conductivity ( $\sigma_{\text{g.b.}}$ ) can all be calculated by Eqs. (5)–(8). In the low-frequency part, the fitted semicircle for the grain boundary overlaps with the extrapolation of the one that would be obtained for the electrode interface under wet conditions. The latter, however, cannot be fitted correctly because there are not enough experimental data points to achieve a reliable semicircular fit. Therefore, less data, but

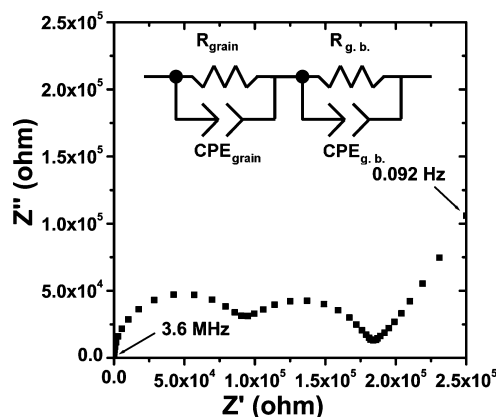


Fig. 4. A typical complex impedance plot of as-fired Sc-BCTZ ceramic at higher frequencies. The inset is an effective electrical equivalent circuit model consisting of grain and grain-boundary components.

still sufficient data points from the grain-boundary arc in Fig. 5(a) are used to extract impedance data that appear reliable. Fitting results of specimens reoxidized in dry/moist atmosphere are shown in Figs. 5(a) and (b). Errors, calculated by  $\Delta_{\text{real}} = (Z'_{\text{fit}} - Z'_{\text{mes}})/|Z^*|$  and  $\Delta_{\text{img}} = (Z''_{\text{fit}} - Z''_{\text{mes}})/|Z^*|$ , range over  $-3\%$ – $3\%$  in the fitting frequency range. This means that the quantitative goodness for fitting was found to be typically between 97% and 98%. Therefore, it is considered that the proposed effective electrical equivalent circuit model successfully represents the Sc-BCTZ ceramics.

Figure 6(a) and (b) show the reciprocal values of grain and grain-boundary capacitance versus temperature that were obtained from nonlinear least-squares (NLLS) fitting of the impedance data. For all specimens, the capacitance of the grain follows the Curie–Weiss law, with the extrapolated Curie–Weiss temperature ( $T_0$ ) ranging from 61°C to 65°C. This is consistent with values reported in an earlier study.<sup>40</sup> The calculated Curie–Weiss constant were  $1.1\text{E}+5$ – $1.8\text{E}+5\text{K}$ , which are in close agreement with that of bulk BaTiO<sub>3</sub>,  $\sim 1.5\text{E}+5\text{K}$ .<sup>41</sup> The reciprocal values of grain-boundary capacitance are approximately constant or do very slightly increase with the increase in temperature, which is similar to the behavior of the constriction boundary model.<sup>42</sup> These results show that the evaluated  $R$  and  $C$  values of grain and grain boundary are quite reasonable in the above effective electrical equivalent circuit model.

Figure 7(a) and (b) show the grain and grain-boundary conductivity versus the inverse absolute temperature for Sc-BCTZ ceramics sintered in moist reducing atmosphere and subsequently reoxidized at 1000°C in various moist and dry atmospheres. The data were obtained from the fitting of the impedance data and using Eqs. (6) and (8). Both the grain and grain-boundary conductivity of all specimens show roughly an Arrhenius-type behavior. The grain and grain-boundary conductivity are approximately consistent for

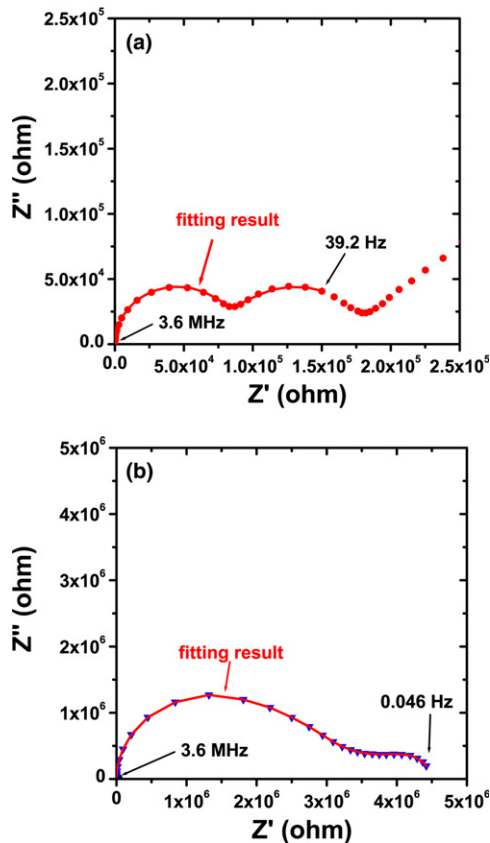


Fig. 5. Fitting results of (a) additionally reoxidized in moist N<sub>2</sub> with 50 ppm O<sub>2</sub> (b) additionally reoxidized in dry N<sub>2</sub> with 50 ppm O<sub>2</sub> using proposed effective electrical equivalent circuit model.

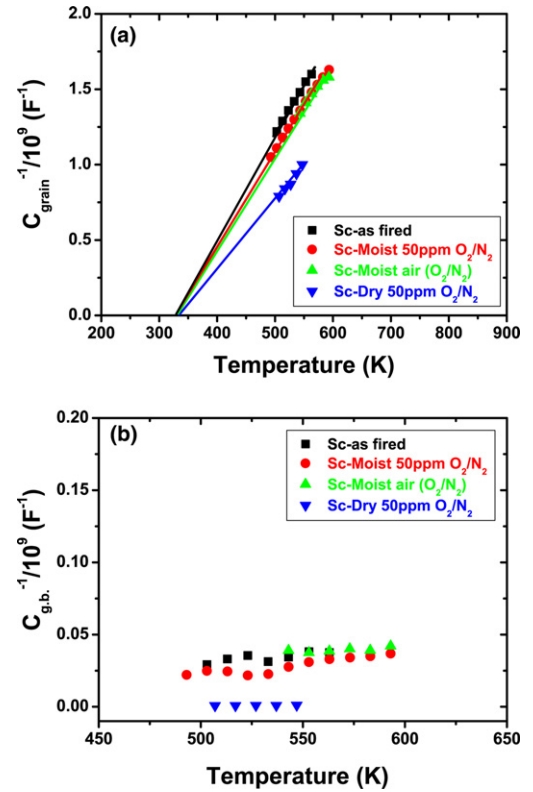


Fig. 6. Reciprocal values of (a) grain and (b) grain-boundary capacitance versus temperature that were obtained from the NLLS fitting of the impedance data for Sc-BCTZ ceramics sintered in moist reducing atmosphere (black open circle) and reoxidized in various dry and moist atmospheres (colored closed geometrical patterns).

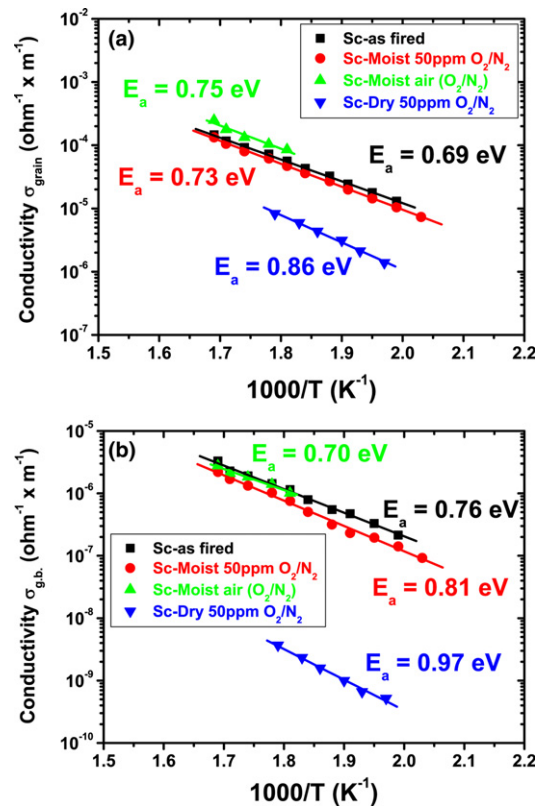


Fig. 7. (a) Grain and (b) grain-boundary conductivity versus inverse temperature for Sc-BCTZ ceramics sintered in moist reducing atmosphere (black open circle) and reoxidized in various dry and moist atmospheres (colored closed symbols).

Sc-BCTZ ceramics sintered in moist reducing and additionally reoxidized samples in moist atmosphere at the same measurement temperatures. On the other hand, when Sc-BCTZ ceramics are reoxidized in dry  $N_2$  with 50 ppm  $O_2$  both the grain and grain-boundary conductivity decrease systematically at the same measurement temperatures. One can find that the behavior of the electrical conductivity in grain and grain boundary is in agreement with these observations: (1) higher conductivity under wet than dry conditions. (2) Grain and grain-boundary conductivity are essentially independent of the partial oxygen pressure under wet conditions. Both two observations mentioned above deduce that hydroxyl defects are the dominant charge carriers over the whole temperature range of 200°C–350°C under wet conditions in this study, which is in a good accordance to observations in the low temperature region (<400°C) by S. M. H. Rahman et al.<sup>43</sup> It can be noticed that the grain-boundary conductivity for Sc-BCTZ treated in dry atmosphere is observed to be about three orders of magnitude lower than that of Sc-BCTZ reoxidized in wet atmosphere. This result infers that the presence of hydroxyl defects ( $OH^{\bullet}_O$ ) during reoxidation may dominate not only to the change in grain conduction, but also the grain-boundary conduction.

Moreover, a difference between wet and dry reoxidation was also observed in the activation energies of grain and grain-boundary conductivity, suggesting a change in the dominating conduction mechanism. It is well-known<sup>44</sup> that the electrical conductivity, in  $BaTiO_3$ , consists of electronic conductivity ( $\sigma_{elec}$ ) and ionic conductivity ( $\sigma_{ion}$ ). Thus, the total conductivity is the sum of these contributions:

$$\sigma = \sigma_{electron} + \sigma_{ion} \quad (9)$$

The cation  $Ti^{3+}$ , if present, acts like an electron donor, ready to provide electrons for electronic conduction, while  $O^{2-}$  ions may also diffuse via the vacancies for ionic conduction. For pure  $BaTiO_3$ , electronic conduction is dominant for temperatures up to 500°C, but ionic conduction of oxygen vacancy becomes significant at about 1000°C. Proton hopping is assumed to give rise to a considerable contribution to the ionic conduction in ceramics, in addition to electromobility of oxygen vacancies. Reoxidation in dry atmosphere causes desorption of water and removal of protons from the grains and out of the grain boundaries. The elimination of protons lowers the additional ionic conductivity inside the grains and the surrounding grain boundaries. As a result, the grain conductivity in Sc-BCTZ reoxidized in dry atmosphere is most likely preferentially contributed by the motion of electrons. On the other hand, the activation energy of the grain conductivity, determined from the moist as-fired and reoxidized specimens, decreases to  $E_a = 0.69$ – $0.75$  eV. Su et al.<sup>20</sup> found comparable values  $E_a = 0.75$ – $0.76$  eV for grain conductivity of Y-BCTZ that was pretreated in wet atmosphere. This variation suggests that the grain conduction in wet atmosphere might be determined by hydroxyl defects ( $OH^{\bullet}_O$ ).

#### (4) Dielectric Effects

Figure 8 shows the bulk dielectric constant of the Sc-BCTZ ceramics at 1 kHz as a function of temperature. The frequency dependence of the dielectric constant was not systematically studied. However, there were no major changes of the dielectric constant observed in the frequency range 0.1–100 kHz. Former studies of acceptor-doped BCTZ revealed a slight frequency dependence of the dielectric constant, but a large variation in  $\tan\delta$ , similar as observed in Sc-doped BCTZ dielectric material.<sup>19</sup> All data fall on a single Curie peak yielding in a ferroelectric phase transition at  $T_C = -12^\circ\text{C}$ . A relatively small difference was found in the ferroelectric range below  $T_C$ . The large change in dielectric

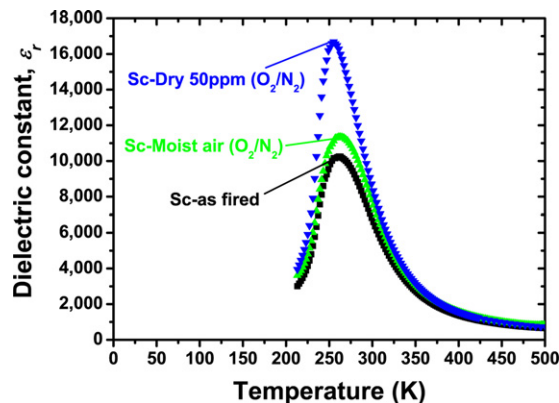


Fig. 8. Bulk dielectric temperature characteristic for Sc-BCTZ ceramics sintered in moist reducing atmosphere and reoxidized in various dry and moist atmospheres.

constant at  $T_C$  from the moist reduced to the dry reoxidized state might be attributed to annihilation of protons. Complexes of acceptor ions and protons may reduce the mobility of ferroelectric domains, thus diminishing dielectric constant in the ferroelectric region.<sup>45</sup> It is interesting to note that significant differences regarding the height of the Curie maxima between specimens reoxidized in dry and in moist atmospheres were observed. In the case of dry atmospheres, the dielectric maxima are enhanced by more than 45% compared to as-fired samples in moist atmosphere. The differences in the height of the dielectric maxima around the Curie point were not only observed in Sc-BCTZ, but also in many other acceptor-doped BCTZ ceramics.<sup>19,20</sup> The effect is clearly ascribed to a proton effect. It seems therefore quite reasonable that the effect is caused by an interaction of protons and acceptors or protons and domain walls. A further study is required in the same material system to verify this behavior.

On the other hand, a considerable difference between  $T_C$  and  $T_0$  was found in this study. It should be noted that Sc-BCTZ ceramics containing 18 mol% of Zr show a strong diffuse temperature dependence of the dielectric constant, which could be attributed to a second-order phase transition. In this case, the application of Curie–Weiss equation with the physical parameter of  $T_0$  as the critical temperature and the Curie–Weiss constant  $C$  might give deviating results compared to materials which follow first-order behavior, such as pure coarse-grained ferroelectric  $BaTiO_3$  ceramics. Another possible reason for the deviation between  $T_C$  and  $T_0$  of Sc-BCTZ ceramics is that the analysis of Curie–Weiss temperature  $T_0$  only refers to the bulk contribution of the dielectric constant, extracted from impedance data,<sup>46</sup> whereas the experimental determination  $T_C$  relies on the temperature dependence of the overall net dielectric constant.

#### IV. Summary and Conclusions

This study considered in detail the influence of hydroxyl defects ( $OH^{\bullet}_O$ ) in Sc-BCTZ on the electrical conduction behavior. Bulk dielectric materials with an average grain size of approximately 5  $\mu\text{m}$  were obtained by sintering in a moist reducing atmosphere and subsequent reoxidation in dry or moist atmospheres.

Impedance spectroscopy was utilized to give a further insight into the bulk characteristic in this system, where grain and grain-boundary contributions are detected at higher frequencies. Through an equivalent circuit model, quantification of grain conductivity and grain-boundary conductivity in the bulk regions of Sc-BCYZ ceramics was obtained. From the impedance analysis, we were able to determine the details of the electrical characteristics for different firing conditions.



During firing or reoxidizing, these dielectric ceramics obviously absorb small amounts of water in moist atmospheres. Water vapor obviously results in the formation of charged hydroxyl defects (OH)<sub>O</sub><sup>•</sup> with oxygen vacancies on regular oxygen sites in the bulk. Protons' hopping in the oxygen sublattice then induces ionic conductivity additional to that of charged oxygen vacancies in the dielectric material. The variation in activation energies between specimens treated in dry and moist conditions suggests that the grain and grain-boundary conductivity are strongly influenced by hydroxyl defects (OH)<sub>O</sub><sup>•</sup>. Moreover, the negligible difference between Sc-BCTZ ceramics sintered in moist reducing and additionally reoxidized in moist atmosphere suggests that heating in moist atmospheres preserve hydroxyl defect (OH)<sub>O</sub><sup>•</sup> from annihilation.

The height of the dielectric maximum at the Curie point is substantially decreased by reoxidation in moist atmosphere. The root cause of this alternation is still unexplained, but it is obviously caused by the proton effect. It seems that interactions of hydroxyl defects with acceptors and domain walls more likely play a key role.

## References

- <sup>1</sup>S. AMJH, "Defect Chemistry and Electrical Transport Properties of Barium Titanate," *Philips Res. Rpts.*, Suppl 3, 1–84 (1974).
- <sup>2</sup>J. Daniels, "Defect Chemistry and Electrical Conductivity of Doped Barium Titanate: 2. Defect Equilibria in Acceptor-Doped Barium Titanate," *Philips Res. Rpts.*, 31 [6] 505–15 (1976).
- <sup>3</sup>J. M. Herbert, "High Permittivity Ceramics Sintered in Hydrogen," *Trans. Brit. Ceram. Soc.*, 62 [8] 645–53 (1963).
- <sup>4</sup>R. Waser, "Electrochemical Boundary Conditions for Resistance Degradation of Doped Alkaline-Earth Titanates," *J. Am. Ceram. Soc.*, 72 [12] 2234–40 (1989).
- <sup>5</sup>H. J. Hagemann, S. Hünten, R. Weirnicke, W. Noorlander, and G. J. Klomp, "Verfahren zur Herstellung eines Dielektrikums," European Patent 82291198.7, 24. September (1982).
- <sup>6</sup>H. J. Hagemann and D. F. Hennings, "Reversible Weight Change of Acceptor Doped Barium Titanate," *J. Am. Ceram. Soc.*, 64 [10] 590–4 (1981).
- <sup>7</sup>M. R. Opitz, K. Albertsen, J. J. Beeson, D. F. Hennings, J. L. Routbort, and C. A. Randall, "Kinetic Process of Base Metal Technology BaTiO<sub>3</sub>-Based Multilayer Capacitors," *J. Am. Ceram. Soc.*, 86 [11] 1879–84 (2004).
- <sup>8</sup>Y. Sakabe, "Dielectric Materials for Base-Metal Multilayer Ceramic Capacitors," *J. Am. Ceram. Soc.*, 66 [9] 1338–41 (1987).
- <sup>9</sup>D. F. Hennings and H. Schreinemacher, "Ca-Acceptors in Dielectric Ceramics, Sintered in Reducing Atmosphere," *J. Eur. Ceram. Soc.*, 15 [8] 795–800 (1995).
- <sup>10</sup>W. S. Lee, W. A. Groen, H. Schreinemacher, and D. F. Hennings, "Dy-Doped Dielectric Material for Sintering in Reducing Atmosphere," *J. Electroceram.*, 5 [1] 31–6 (2000).
- <sup>11</sup>S. Sato, Y. Nakano, A. Sato, and T. Nomura, "Effect of Y-Doping on Resistance Degradation of Multilayer Ceramic Capacitors With Ni Electrodes Under Highly Accelerated Life Test," *Jpn. J. Appl. Phys.*, 36 [9B] 6016–20 (1997).
- <sup>12</sup>M. Li, A. Feteira, and D. C. Sinclair, "Origin of the High Permittivity in (La<sub>0.4</sub>Ba<sub>0.4</sub>Ca<sub>0.2</sub>)(Mn<sub>0.4</sub>Ti<sub>0.6</sub>)O<sub>3</sub> Ceramics," *J. Appl. Phys.*, 98, 84101, 6pp (2005).
- <sup>13</sup>D. F. Hennings, C. Pithan, C. Hofer, and R. Meyer, "Impedance Analysis of BME Dielectric Ceramics," pp. 319–28 in *Ceramic Transactions*, Vol. 167, Developments in Dielectric Materials and Electronic Devices: Proceedings of the 106th Annual Meeting of the American Ceramic Society. Edited by K. M. Nair, R. Guo, A. S. Bhalla, S.-I. Hofer, R. Meyer and C. Pithan. American Ceramic Society, Indianapolis, Indiana, 2004.
- <sup>14</sup>G. Y. Yang, et al., "Oxygen Nonstoichiometry and Dielectric Evolution of BaTiO<sub>3</sub>. Part I – Insulation Resistance Degradation Under Applied DC Bias," *J. Appl. Phys.*, 96 [12] 7500–8 (2004).
- <sup>15</sup>P. Couřová, J. Novák, and N. Hlasivcová, "Hydroxyl as a Defect of the Perovskite BaTiO<sub>3</sub> Lattice," *J. Chem. Phys.*, 45 [9] 3171–4 (1966).
- <sup>16</sup>S. Stotz and C. Wagner, "The Solubility of Water Vapor and Hydrogen in Solid Oxides," *Ber. Bunsen. Phys. Chem.*, 70 [8] 781–8 (1966).
- <sup>17</sup>D. F. Hennings and B. S. Schreinemacher, "Characterization of Hydrothermal Barium Titanate," *J. Eur. Ceram. Soc.*, 9 [1] 41–6 (1992).
- <sup>18</sup>R. Waser, "Solubility of Hydrogen Defects in Doped and Undoped BaTiO<sub>3</sub>," *J. Am. Ceram. Soc.*, 71 [1] 58–63 (1988).
- <sup>19</sup>P. Hansen, D. F. Hennings, and H. Schreinemacher, "Dielectric Properties of Acceptor-Doped (Ba,Ca)(Ti,Zr)O<sub>3</sub> Ceramics," *J. Electrocer.*, 2 [2] 85–94 (1998).
- <sup>20</sup>C. Y. Su, C. Pithan, D. F. Hennings, and R. Waser, "Proton Defects in BaTiO<sub>3</sub>: New Aspects Regarding the Re-Oxidation of Dielectric Materials Fired in Reducing Atmospheres," *J. Eur. Ceram. Soc.*, 33 [15–16] 3007–13 (2013).
- <sup>21</sup>R. Waser, T. Baiatu, and K. H. Härdtl, "DC Electrical Degradation of Perovskite Type Titanates: I Ceramics," *J. Am. Ceram. Soc.*, 73 [6] 1645–53 (1990).
- <sup>22</sup>K. D. Kreuer, St. Adams, W. Münch, A. Fuchs, U. Klock, and J. Maier, "Proton Conducting Alkaline Earth Zirconates and Titanates for High Drain Electrochemical Applications," *Solid State Ionics*, 145, 295–306 (2001).
- <sup>23</sup>Y. Tsur, T. D. Dunbar, and C. A. Randall, "Crystal and Defect Chemistry of Rare-Earth Cations in BaTiO<sub>3</sub>," *J. Electrocerm.*, 73 [1–4] 25–34 (2001).
- <sup>24</sup>G. V. Lewis and C. R. A. Catlow, "Computer Modeling of Barium Titanate," *Radiat. Effects*, 7 [1] 307–14 (1983).
- <sup>25</sup>G. V. Lewis and C. R. A. Catlow, "Defect Studies of Doped and Undoped Barium Titanate Using Computer Simulation Techniques," *J. Phys. Chem. Sol.*, 47 [1] 89–97 (1986).
- <sup>26</sup>Y. Tsur, A. Hitomi, I. Scrymgeour, and C. A. Randall, "Site Occupancy of Rare-Earth Cations in BaTiO<sub>3</sub>," *Jpn. J. Appl. Phys.*, 40 [1–1] 255–8 (2001).
- <sup>27</sup>H. Kishi, Y. Mizuno, and H. Chazono, "Base-Metal Electrode-Multilayer Ceramic Capacitors: Past, Present and Future Perspectives," *Jpn. J. Appl. Phys.*, 42 [1–1] 1–15 (2003).
- <sup>28</sup>H. Kishi, N. Kohzu, J. Sugino, H. Ohsato, Y. Iguchi, and T. Okuda, "The Effect of Rare-Earth (La, Sm, Dy, Ho and Er) and Mg on the Microstructure in BaTiO<sub>3</sub>," *J. Eur. Ceram. Soc.*, 19 [6–7] 1043–6 (1999).
- <sup>29</sup>R. D. Shannon, "Revised Effective Ionic Radii and Systematic Studies of Inter-Atomic Distances in Halides and Chalcogenides," *Acta Crystallogr.*, 32, 751–67 (1976).
- <sup>30</sup>H. Katsu, "Crystal- and Defect-Chemistry of Fine Grained Thermistor Ceramics on BaTiO<sub>3</sub> Basis With BaO-Excess," Ph. D. thesis, RWTH Aachen University, Templergraben, 2011.
- <sup>31</sup>J. T. S. Irvine, D. C. Sinclair, and A. R. West, "Electroceramics: Characterization by Impedance Spectroscopy," *Adv. Mat.*, 2 [3] 132–8 (1990).
- <sup>32</sup>J. Jamnik and J. Maier, "Treatment of the Impedance of Mixed Conductors Equivalent Circuit Model and Explicit Approximate Solutions," *J. Electrochem. Soc.*, 146 [11] 4183–8 (1999).
- <sup>33</sup>K. Kaneda, S. Lee, N. J. Donnelly, W. Qu, C. A. Randall, and Y. Mizuno, "Kinetics of Oxygen Diffusion Into Multilayer Ceramic Capacitors During the Re-Oxidation Process and its Implications on Dielectric Properties," *J. Am. Ceram. Soc.*, 94 [11] 3934–40 (2011).
- <sup>34</sup>D. C. Sinclair and A. R. West, "Impedance and Modulus Spectroscopy of Semiconducting BaTiO<sub>3</sub> Showing Positive Temperature Coefficient of Resistance," *J. Appl. Phys.*, 66 [8] 3850–6 (1989).
- <sup>35</sup>I. M. Hodge, M. D. Ingram, and A. R. West, "Impedance and Modulus Spectroscopy of Polycrystalline Solid Electrolytes," *J. Electroanal. Chem.*, 74 [2] 125–43 (1976).
- <sup>36</sup>J. P. Heath, J. S. Dean, J. H. Harding, and D. C. Sinclair, "Simulation of Impedance Spectra for Core-Shell Grain Structures Using Finite Element Modeling," *J. Am. Ceram. Soc.*, 98 [6] 1925–31 (2015).
- <sup>37</sup>M. Kessel, R. A. De Souza, H. I. Yoo, and M. Martin, "Strongly Enhanced Incorporation of Oxygen Into Barium Titanate Based Multilayer Ceramic Capacitors Using Water Vapor," *Appl. Phys. Lett.*, 97 [2] 021910, 3pp (2010).
- <sup>38</sup>X. Guo and J. Maier, "Grain Boundary Blocking Effect in Zirconia: A Schottky Barrier Analysis," *J. Electrochem. Soc.*, 148 [3] E121–6 (2001).
- <sup>39</sup>J. R. Macdonald and W. R. Kenan, *Impedance Spectroscopy: Emphasizing Solid Materials and Systems*. pp. 1–20. John Wiley & Sons, Inc., New York, 1987.
- <sup>40</sup>D. Hennings, A. Schnell, and G. Simon, "Diffuse Ferroelectric Phase Transitions in Ba(Ti<sub>1-x</sub>Zr<sub>x</sub>)O<sub>3</sub> Ceramics," *J. Am. Ceram. Soc.*, 65 [11] 539–44 (1982).
- <sup>41</sup>J. C. Slater, "The Lorentz Correction in Barium Titanate," *Phys. Rev.*, 78 [6] 748–61 (1950).
- <sup>42</sup>N. Hirose and A. R. West, "Impedance Spectroscopy of Undoped BaTiO<sub>3</sub> Ceramics," *J. Am. Ceram. Soc.*, 79 [6] 1633–41 (1996).
- <sup>43</sup>S. M. H. Rahman, I. Ahmed, R. Haugsrud, S. G. Eriksson, and C. S. Knee, "Characterisation of Structure and Conductivity of BaTi<sub>0.9</sub>Sc<sub>0.1</sub>O<sub>3-δ</sub>," *Solid State Ionics*, 255, 140–6 (2014).
- <sup>44</sup>K. C. Kao, *Dielectric Phenomena in Solids: With Emphasis on Physical Concept of Electronic Process*; pp. 226–7. Academic Press, San Diego, California, 2004.
- <sup>45</sup>H. Dederichs and G. Arlt, "Aging of Fe-Doped PZT Ceramics and the Domain Wall Contribution to the Dielectric Constant," *Ferroelectrics*, 68 [1] 281–92 (1986).
- <sup>46</sup>A. Yu. Emelyanov, N. A. Pertsev, S. Hoffmann-Eifert, U. Bottger, and R. Waser, "Grain-Boundary Effect on the Curie-Weiss Law of Ferroelectric Ceramics and Polycrystalline Thin Films: Calculation by the Method of Effective Medium," *J. Electrochem. Soc.*, 9 [1] 5–16 (2002). □